

Find  $\tilde{\mathbf{u}}_K \in \mathbf{H}^1(\Omega_K)$ ,  $\tilde{\mathbf{u}}_K|_{\partial\Omega_K \cap (\Omega \cup \Gamma_u)} = \mathbf{U} \in \mathbf{H}^1(\Omega)$ , such that

$$\int_{\Omega_K} \nabla \mathbf{v}_K : \tilde{\boldsymbol{\sigma}}_K d\Omega = \int_{\Omega_K} \mathbf{f} \cdot \mathbf{v}_K d\Omega + \int_{\partial\Omega_K \cap \Gamma_t} \mathbf{t} \cdot \mathbf{v}_K dA \quad (6.9)$$

$\forall \mathbf{v}_K \in \mathbf{H}^1(\Omega_K)$ ,  $\mathbf{v}_K|_{\partial\Omega_K \cap (\Omega \cup \Gamma_u)} = \mathbf{0}$ .

A specific choice for  $\mathbf{U}$  will also be given momentarily. The individual subdomain solutions form an approximate solution to the globally exact problem,  $\mathbf{u}$ . This approximate solution is constructed by a direct assembly process

$$\tilde{\mathbf{u}} \stackrel{\text{def}}{=} \mathbf{U} + (\tilde{\mathbf{u}}_1 - \mathbf{U})|_{\Omega_1} + (\tilde{\mathbf{u}}_2 - \mathbf{U})|_{\Omega_2} + \dots + (\tilde{\mathbf{u}}_N - \mathbf{U})|_{\Omega_N}. \quad (6.10)$$

The approximate displacement field is continuous, however, the approximate traction field is usually discontinuous. Clearly, if there are no jumps in the tractions, the solution is exact.

### 6.6.2 Relation to the material tests

We have for any kinematically admissible function  $\mathbf{w}$ , using the (bilinear operator) notation,

$$0 \leq \|\mathbf{u} - \mathbf{w}\|_{E(\Omega)}^2 = \mathcal{B}(\mathbf{u} - \mathbf{w}, \mathbf{u} - \mathbf{w}) = 2\mathcal{J}(\mathbf{w}) - 2\mathcal{J}(\mathbf{u}) \Rightarrow \mathcal{J}(\mathbf{u}) \leq \mathcal{J}(\mathbf{w}),$$

where  $\mathcal{J}(\mathbf{w}) \stackrel{\text{def}}{=} \frac{1}{2}\mathcal{B}(\mathbf{w}, \mathbf{w}) - \mathcal{F}(\mathbf{w})$ . In other words, the true solution has a minimum potential (PMPE). By applying the PMPE, for the test loading  $\mathbf{u}|_{\partial\Omega} = \mathcal{E} \cdot \mathbf{x} = \mathbf{d}$ ,  $\mathbf{f} = \mathbf{0}$ , with the specific (kinematically admissible) choice  $\mathbf{w} = \mathbf{U}$ , we obtain  $\|\mathbf{u} - \mathbf{U}\|_{E(\Omega)}^2 = 2(\mathcal{J}(\mathbf{U}) - \mathcal{J}(\mathbf{u})) \Rightarrow \mathcal{J}(\mathbf{u}) = \mathcal{J}(\mathbf{U}) - \frac{1}{2}\|\mathbf{u} - \mathbf{U}\|_{E(\Omega)}^2$ .

*The critical observation is that when choosing  $\mathbf{w} = \mathbf{U} \stackrel{\text{def}}{=} \mathcal{E} \cdot \mathbf{x}$  in Box 6.9, then  $\tilde{\mathbf{u}}$ , as defined in eq. 6.10, is also kinematically admissible.* Therefore, we have by direct expansion  $\|\mathbf{u} - \tilde{\mathbf{u}}\|_{E(\Omega)}^2 = 2(\mathcal{J}(\tilde{\mathbf{u}}) - \mathcal{J}(\mathbf{u})) = 2(\mathcal{J}(\tilde{\mathbf{u}}) - \mathcal{J}(\mathbf{U})) + \|\mathbf{u} - \mathbf{U}\|_{E(\Omega)}^2$ . Since  $\tilde{\mathbf{u}}_K$  is a solution to a subdomain boundary value problem posed over  $\Omega_K$ , it minimizes the corresponding subdomain potential energy function  $\mathcal{J}_K(\cdot)$ . Therefore,  $\mathcal{J}(\mathbf{U}) = \sum_{K=1}^S \mathcal{J}_K(\mathbf{U}) \geq \sum_{K=1}^S \mathcal{J}_K(\tilde{\mathbf{u}}_K) = \mathcal{J}(\tilde{\mathbf{u}})$ . Consequently,

$$\|\mathbf{u} - \tilde{\mathbf{u}}\|_{E(\Omega)}^2 = \underbrace{2(\mathcal{J}(\tilde{\mathbf{u}}) - \mathcal{J}(\mathbf{U}))}_{\text{negative}} + \|\mathbf{u} - \mathbf{U}\|_{E(\Omega)}^2. \quad (6.11)$$

By direct expansion we have  $\|\mathbf{u} - \mathbf{U}\|_{E(\Omega)}^2 = \mathcal{E} : (\langle \mathbf{IE} \rangle - \mathbf{IE}^*) : \mathcal{E}|\Omega| \leq \mathcal{E} : (\langle \mathbf{IE} \rangle - \langle \mathbf{IE}^{-1} \rangle^{-1}) : \mathcal{E}|\Omega|$ . We have by definition,  $2\mathcal{J}(\mathbf{u}) = \mathcal{E} : \mathbf{IE}^* : \mathcal{E}|\Omega|$ ,  $2\mathcal{J}(\mathbf{U}) = \mathcal{E} : \langle \mathbf{IE} \rangle : \mathcal{E}|\Omega|$ , and  $2\mathcal{J}_K(\tilde{\mathbf{u}}) = \mathcal{E} : \mathbf{IE}_K^* : \mathcal{E}|\Omega_K|$ , which implies  $2\mathcal{J}(\tilde{\mathbf{u}}) = \mathcal{E} : \tilde{\mathbf{IE}}^* : \mathcal{E}|\Omega|$ . By direct substitution this completes the first of the

Now partition the domain into  $S$  subdomains,  $\Omega = \cup_{K=1}^S \Omega_K$ . The pieces do not have to be the same size or shape, although for illustration purposes it is convenient to take a uniform (regular) partitioning (Figure 7.2). Consider a kinematically admissible function,  $\mathbf{U} \in \mathbf{H}^1(\Omega)$  and  $\mathbf{U}|_{\Gamma_u} = \mathbf{d}$ , which is projected onto the *internal boundaries* ( $\partial\Omega_K$ ) of the subdomains. Any subdomain boundaries coinciding with the exterior surface retain their original boundary conditions (Figure 7.2). Accordingly, we have the following virtual work formulation, for each subdomain,  $1 \leq K \leq S$ :

Find  $\tilde{\mathbf{u}}_K \in \mathbf{H}^1(\Omega_K)$ ,  $\tilde{\mathbf{u}}_K|_{\partial\Omega_K \cap (\Omega \cup \Gamma_u)} = \mathbf{U} \in \mathbf{H}^1(\Omega)$ , such that

$$\int_{\Omega_K} \nabla \mathbf{v}_K : \underbrace{\mathbf{IE} : \nabla \tilde{\mathbf{u}}_K}_{\tilde{\boldsymbol{\sigma}}_K} d\Omega = \int_{\Omega_K} \mathbf{f} \cdot \mathbf{v}_K d\Omega + \int_{\partial\Omega_K \cap \Gamma_t} \mathbf{t} \cdot \mathbf{v}_K dA \quad (7.13)$$

$\forall \mathbf{v}_K \in \mathbf{H}^1(\Omega_K)$ ,  $\mathbf{v}_K|_{\partial\Omega_K \cap (\Omega \cup \Gamma_u)} = \mathbf{0}$ .

The individual subdomain solutions,  $\tilde{\mathbf{u}}_K$ , are zero outside of the corresponding subdomain  $\bar{\Omega}_K$ . In this case the approximate solution is constructed by a direct assembly process,  $\tilde{\mathbf{u}} \stackrel{\text{def}}{=} \mathbf{U} + (\tilde{\mathbf{u}}_1 - \mathbf{U})|_{\Omega_1} + (\tilde{\mathbf{u}}_2 - \mathbf{U})|_{\Omega_2} + \dots + (\tilde{\mathbf{u}}_S - \mathbf{U})|_{\Omega_S}$ . The approximate displacement field is in  $\mathbf{H}^1(\Omega)$ , however, the approximate traction field is possibly discontinuous. Logical choices of  $\mathbf{U}$ , i.e.  $\mathbf{U} = \mathcal{E} \cdot \mathbf{x}$ , will be given momentarily. It should be clear that if  $\tilde{\mathbf{u}} = \mathbf{u}$  on the internal partition boundaries, then the approximate solution is exact. Since we employ energy type principles to generate approximate solutions, we use an induced energy norm to measure the solution differences

$$0 \leq \|\mathbf{u} - \tilde{\mathbf{u}}\|_{E(\Omega)}^2 \stackrel{\text{def}}{=} \int_{\Omega} \nabla(\mathbf{u} - \tilde{\mathbf{u}}) : \mathbf{IE} : \nabla(\mathbf{u} - \tilde{\mathbf{u}}) d\Omega.$$

It is convenient to cast the error in terms of the potential energy,

$$\mathcal{J}(\mathbf{w}) \stackrel{\text{def}}{=} \frac{1}{2} \int_{\Omega} \nabla \mathbf{w} : \mathbf{IE} : \nabla \mathbf{w} d\Omega - \int_{\Omega} \mathbf{f} \cdot \mathbf{w} d\Omega - \int_{\Gamma_t} \mathbf{t} \cdot \mathbf{w} dA,$$

where  $\mathbf{w}$  is any kinematically admissible function. This leads to

$$\|\mathbf{u} - \mathbf{w}\|_{E(\Omega)}^2 = 2(\mathcal{J}(\mathbf{w}) - \mathcal{J}(\mathbf{u})) \quad \text{or} \quad \mathcal{J}(\mathbf{u}) \leq \mathcal{J}(\mathbf{w})$$

which is a form of the Principle of Minimum Potential Energy. In other words, the true solution possesses a minimum potential. By direct substitution we have  $\|\mathbf{u} - \tilde{\mathbf{u}}\|_{E(\Omega)}^2 = 2(\mathcal{J}(\tilde{\mathbf{u}}) - \mathcal{J}(\mathbf{u}))$ .

In the special case that  $\mathbf{u}|_{\partial\Omega} = \mathcal{E} \cdot \mathbf{x}$ , which is equivalent to testing each subsample with  $\mathbf{u}|_{\partial\Omega_K} = \mathcal{E} \cdot \mathbf{x}$  and  $\mathbf{f} = \mathbf{0}$ , then

$$\|\mathbf{u} - \tilde{\mathbf{u}}\|_{E(\Omega)}^2 = \mathcal{E} : (\tilde{\mathbf{IE}}^* - \mathbf{IE}^*) : \mathcal{E} |\Omega|,$$

where  $\langle \tilde{\boldsymbol{\sigma}} \rangle_{\Omega_K} \stackrel{\text{def}}{=} \tilde{\mathbf{IE}}_K^* : \langle \tilde{\boldsymbol{\epsilon}} \rangle_{\Omega_K}$  and  $\tilde{\mathbf{IE}}^* \stackrel{\text{def}}{=} \sum_{K=1}^S \tilde{\mathbf{IE}}_K^* \frac{|\Omega_K|}{|\Omega|}$ .

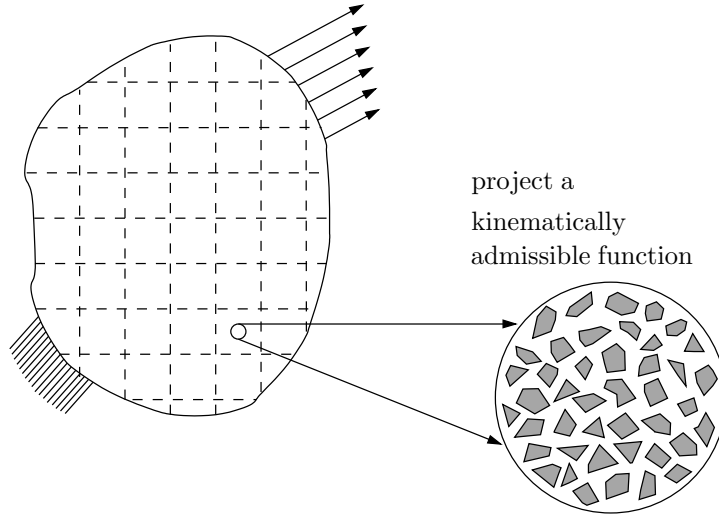


**Fig. 8.1.** Construction of the approximate solution.

To construct the approximate microstructural solutions we first partition the domain,  $\Omega$ , into  $N$  nonintersecting open subdomains  $\cup_{K=1}^N \Omega_K = \overline{\Omega}$ . We define the boundary of an individual subdomain  $\Omega_K$ , as  $\partial\Omega_K$ . When employing the applied internal displacement approach, a kinematically admissible function,  $\mathbf{U} \in \mathbf{H}^1(\Omega)$  and  $\mathbf{U}|_{\Gamma_u} = \mathbf{d}$ , is projected onto the *internal boundaries* of the subdomain partitions. Any subdomain boundaries coinciding with the exterior surface retain their original boundary conditions (Figure 8.1). Accordingly, we have the following virtual work formulation, for each subdomain,  $1 \leq K \leq N$  :

$$\begin{array}{l}
 \text{Find } \tilde{\mathbf{u}}_K \in \mathbf{H}^1(\Omega_K), \tilde{\mathbf{u}}_K|_{\partial\Omega_K \cap (\Omega \cup \Gamma_u)} = \mathbf{U} \in \mathbf{H}^1(\Omega), \text{ such that} \\
 \int_{\Omega_K} \nabla \mathbf{v}_K : \tilde{\boldsymbol{\sigma}}_K \, d\Omega = \int_{\Omega_K} \mathbf{f} \cdot \mathbf{v}_K \, d\Omega + \int_{\partial\Omega_K \cap \Gamma_t} \mathbf{t} \cdot \mathbf{v}_K \, dA \\
 \forall \mathbf{v}_K \in \mathbf{H}^1(\Omega_K), \mathbf{v}_K|_{\partial\Omega_K \cap (\Omega \cup \Gamma_u)} = \mathbf{0}.
 \end{array} \quad (8.2)$$

The constitutive law and microstructure are identical to that of the globally exact problem. In the infinitesimal strain, linearly elastic, case  $\tilde{\boldsymbol{\sigma}} = \mathbf{IE} : \nabla \tilde{\mathbf{u}}_K$ . The individual subdomain solutions,  $\tilde{\mathbf{u}}_K$ , are zero outside of the corresponding subdomain  $\overline{\Omega}_K$ . In this case the approximate solution is constructed by a direct assembly process

$$\tilde{\mathbf{u}} \stackrel{\text{def}}{=} \mathbf{U} + (\tilde{\mathbf{u}}_1 - \mathbf{U})|_{\Omega_1} + (\tilde{\mathbf{u}}_2 - \mathbf{U})|_{\Omega_2} + \dots + (\tilde{\mathbf{u}}_N - \mathbf{U})|_{\Omega_N}. \quad (8.3)$$

The approximate displacement field is in  $\mathbf{H}^1(\Omega)$ , however, the approximate traction field is possibly discontinuous. Logical choices of  $\mathbf{U}$  will be given later

It is convenient to cast the error in terms of the potential energy for the case of linear elasticity,  $\mathcal{J}(\mathbf{w}) \stackrel{\text{def}}{=} \frac{1}{2} \int_{\Omega} \nabla \mathbf{w} : \mathbf{IE} : \nabla \mathbf{w} \, d\Omega - \int_{\Omega} \mathbf{f} \cdot \mathbf{w} \, d\Omega - \int_{\Gamma_t} \mathbf{t} \cdot \mathbf{w} \, dA$ , where  $\mathbf{w}$  is any kinematically admissible function. The well known relationship for any kinematically admissible function  $\mathbf{w}$  is

$$\|\mathbf{u} - \mathbf{w}\|_{E(\Omega)}^2 = 2(\mathcal{J}(\mathbf{w}) - \mathcal{J}(\mathbf{u})) \text{ or } \mathcal{J}(\mathbf{u}) \leq \mathcal{J}(\mathbf{w}), \quad (8.6)$$

which is the Principle of Minimum Potential Energy (PMPE). In other words, the true solution possesses a minimum potential. Therefore, since  $\tilde{\mathbf{u}}$  is kinematically admissible, we immediately have  $\|\mathbf{u} - \tilde{\mathbf{u}}\|_{E(\Omega)}^2 = 2(\mathcal{J}(\tilde{\mathbf{u}}) - \mathcal{J}(\mathbf{u}))$ . The critical observation is that if we can bound  $\mathcal{J}(\mathbf{u})$  from below, then we can bound the error from above. In other words, what we seek is  $\mathcal{J}^- \leq \mathcal{J}(\mathbf{u})$ .

To bound  $\mathcal{J}(\mathbf{u})$  in terms of easily accessible quantities, we first calculate a computationally inexpensive, kinematically admissible, regularized test solution. The regularized test solution,  $\mathbf{u}^R$ , is characterized by a virtual work formulation:

Find a  $\mathbf{u}^R \in \mathbf{H}^1(\Omega)$ ,  $\mathbf{u}^R|_{\Gamma_u} = \mathbf{d}$ , such that

$$\int_{\Omega} \nabla \mathbf{v} : \boldsymbol{\sigma}^R \, d\Omega = \int_{\Omega} \mathbf{f} \cdot \mathbf{v} \, d\Omega + \int_{\Gamma_t} \mathbf{t} \cdot \mathbf{v} \, dA \quad \forall \mathbf{v} \in \mathbf{H}^1(\Omega), \mathbf{v}|_{\Gamma_u} = \mathbf{0}. \quad (8.7)$$

Here the constitutive law for  $\boldsymbol{\sigma}^R$  should be taken to be as simple as a possible, i.e. a constant (regularized) fourth order symmetric positive definite linear elasticity tensor  $\mathcal{IR}$ , defined via  $\boldsymbol{\sigma}^R = \mathcal{IR} : \nabla \mathbf{u}^R$ . In general, the regularized solution  $(\boldsymbol{\sigma}^R, \mathbf{u}^R)$  does not coincide with the field associated with the decoupling solution  $\mathbf{U}$ . If we choose  $\mathbf{w} = \mathbf{u}^R$  in Equation 8.6, which is an admissible function, we obtain  $\|\mathbf{u} - \mathbf{u}^R\|_{E(\Omega)}^2 = 2(\mathcal{J}(\mathbf{u}^R) - \mathcal{J}(\mathbf{u}))$ , which implies  $\mathcal{J}(\mathbf{u}) = \mathcal{J}(\mathbf{u}^R) - \frac{1}{2}\|\mathbf{u} - \mathbf{u}^R\|_{E(\Omega)}^2$ . Our objective is to form an *upper bound* on  $\|\mathbf{u} - \mathbf{u}^R\|_{E(\Omega)}$  in terms of  $\mathcal{IR}$ ,  $\mathbf{IE}$  and  $\nabla \mathbf{u}^R$ , to obtain a *lower bound* on  $\mathcal{J}(\mathbf{u})$ . For the bound to be useful, it should contain no unknown constants, and should be solely in terms of the regularized solution and the material data. In other words we seek  $\|\mathbf{u} - \mathbf{u}^R\|_{E(\Omega)} \leq \mathcal{H}^{+(u)}$ , which will lead to

$$\mathcal{J}^- \stackrel{\text{def}}{=} \mathcal{J}(\mathbf{u}^R) - \frac{1}{2}(\mathcal{H}^{+(u)})^2 \leq \mathcal{J}(\mathbf{u}),$$

thus supplying an upper bound for the quantities in Box 8.5.

### 8.2.1 Multiscale proximity bounds

The solution corresponding to a material with microstructure is  $\mathbf{u}$ , and is characterized by the following virtual work formulation:

Find  $\mathbf{u} \in \mathbf{H}^1(\Omega)$ ,  $\mathbf{u}|_{\Gamma_u} = \mathbf{d}$ , such that

$$\underbrace{\int_{\Omega} \nabla \mathbf{v} : \boldsymbol{\sigma} \, d\Omega}_{\stackrel{\text{def}}{=} \mathcal{B}(\mathbf{u}, \mathbf{v})} = \underbrace{\int_{\Omega} \mathbf{f} \cdot \mathbf{v} \, d\Omega + \int_{\Gamma_t} \mathbf{t} \cdot \mathbf{v} \, dA}_{\stackrel{\text{def}}{=} \mathcal{F}(\mathbf{v})} \quad \forall \mathbf{v} \in \mathbf{H}^1(\Omega), \mathbf{v}|_{\Gamma_u} = \mathbf{0}. \quad (8.8)$$

up the solution process. In other words, a starting vector that captures a-priori the "long wave" components (low frequency eigenmodes) of the solution is advantageous. This increases the effectiveness of the CG searches for this class of problems. A well known fact with regard to iterative solvers is the fact that they are quite adept at capturing high-frequency responses. However, they typically may require many iterations to capture "long-wave" modes. For a discussion see Briggs [18]. For this decomposition, since the number of CG iterations to solve each subdomain problem was  $m_{loc} \approx 49$  (Table 6.4). Therefore, the cost to solve all of the subdomain problems was  $m_{loc}(\frac{n}{N})^2 N \approx 49 \frac{n^2}{512}$ , as opposed to the direct cost of approximately  $M_{glob} n^2$ , where  $M_{glob} > m_{loc}$ . In this case the approximate cost savings are approximately  $DIRECT COSTS/DECOMPOSED COSTS \approx \frac{N M_{glob}}{m_{loc}} \geq 512$ . The time to preprocess, solve and postprocess each 20 particle subdomain took no more than one minute on a single RISC 6000 workstation. Clearly, the overall solution process is trivially parallelizable.

We computed the following upper bound, which coincided with the previous chapter's results, normalized by the energy of  $\mathbf{U} = \mathcal{E} \cdot \mathbf{x}$ , on the error

$$0 \leq \frac{\|\mathbf{u} - \tilde{\mathbf{u}}\|_{E(\Omega)}^2}{\|\mathbf{U}\|_{E(\Omega)}^2} \leq \frac{2(\mathcal{J}(\tilde{\mathbf{u}}) - \mathcal{J}^-)}{\|\mathbf{U}\|_{E(\Omega)}^2} = 0.1073, \quad (8.29)$$

where the maximized lower bound on the potential is

$$\mathcal{J}^- = \frac{1}{2} \mathcal{E} : \langle \mathbf{IE}^{-1} \rangle_{\Omega}^{-1} : \mathcal{E} |\Omega|, \quad (8.30)$$

where  $\mathcal{IR}^* = \langle \mathbf{IE}^{-1} \rangle_{\Omega}^{-1} = \left( \frac{1}{|\Omega|} \int_{\Omega} \mathbf{IE}^{-1} d\Omega \right)^{-1}$ , has been used. The optimal  $\mathcal{IR}^*$  stems from computing  $\frac{\partial \mathcal{J}^-}{\partial \mathcal{IR}} = \mathbf{0}$ ,  $\frac{\partial^2 \mathcal{J}^-}{\partial \mathcal{IR}^2} < \mathbf{0} \Rightarrow \mathcal{IR}^* = \langle \mathbf{IE}^{-1} \rangle_{\Omega}^{-1}$ .

**Remarks:** In the general case, in order to determine the optimal regularization for a given boundary value problem, one must search for the components of  $\mathcal{IR}$  which minimize any one of the estimates derived earlier, which, for the sake of generality, we denote by  $\Pi$ . This entails that boundary value problems must be solved repeatedly to form, for example, a multivariate Newton-type search for the components of  $\mathcal{IR}$  denoted  $R_i$ . Explicitly written, a Newton type system is  $[\mathbf{IH}]\{\Delta \mathcal{IR}\} = -\{\mathbf{g}\}$ , where  $[\mathbf{IH}]$  is the Hessian matrix ( $N \times N$ ), with components  $H_{ij} = \frac{\partial^2 \Pi(\mathcal{IR})}{\partial R_i \partial R_j}$ ,  $\{\mathbf{g}\}$  is the gradient ( $N \times 1$ ), with components  $g_i = \frac{\partial \Pi(\mathcal{IR})}{\partial R_i}$  and where  $\{\Delta \mathcal{IR}\}$  is the increment ( $N \times 1$ ), with components  $\Delta R_i$ , needed to update the components of  $\mathcal{IR}$  (which are initially guessed). To construct the system  $[\mathbf{IH}]\{\Delta \mathcal{IR}\} = -\{\mathbf{g}\}$ ,  $\mathbf{u}^R$  and  $\boldsymbol{\sigma}^R$  must be determined numerically, for example using the finite element method, to determine  $\Pi$  and its derivatives. As with most complicated systems, finite difference approximations of the gradient and Hessian components are constructed with respect to the search parameters by perturbing the search variables around a base point. The reader is referred to Gill et. al [61] for

a fundamental difficulty with such an approach since the space of admissible trial stress functions must satisfy equilibrium,  $\nabla \cdot \boldsymbol{\sigma}^{R,h} + \mathbf{f} = \mathbf{0}$ , and the test functions must be divergence free,  $\nabla \cdot \boldsymbol{\gamma}^h = \mathbf{0}$ . However, formally proceeding we have

$$\|\boldsymbol{\sigma} - \boldsymbol{\sigma}^R\|_{E^{-1}(\Omega)}^2 = 2(\mathcal{K}(\boldsymbol{\sigma}^R) - \mathcal{K}(\boldsymbol{\sigma})), \quad (8.35)$$

and

$$\|\boldsymbol{\sigma} - \boldsymbol{\sigma}^{R,h}\|_{E^{-1}(\Omega)}^2 = 2(\mathcal{K}(\boldsymbol{\sigma}^{R,h}) - \mathcal{K}(\boldsymbol{\sigma})), \quad (8.36)$$

leading to

$$\|\boldsymbol{\sigma} - \boldsymbol{\sigma}^{R,h}\|_{E^{-1}(\Omega)}^2 = \underbrace{\|\boldsymbol{\sigma} - \boldsymbol{\sigma}^R\|_{E^{-1}(\Omega)}^2}_{\text{difference in scales}} + \underbrace{2(\mathcal{K}(\boldsymbol{\sigma}^{R,h}) - \mathcal{K}(\boldsymbol{\sigma}^R))}_{\text{coarse-scale discretization error}}. \quad (8.37)$$

Finally, by adding Equations 8.33 and 8.36 we obtain an exact “mixed estimate” for a solution generated by a standard finite element method ( $H$ ) and a solution generated by a method which generates a statically admissible solution ( $h$ )

$$\|\mathbf{u} - \mathbf{u}^{R,H}\|_{E(\Omega)}^2 + \|\boldsymbol{\sigma} - \boldsymbol{\sigma}^{R,h}\|_{E^{-1}(\Omega)}^2 = 2(\mathcal{J}(\mathbf{u}^{R,H}) + \mathcal{K}(\boldsymbol{\sigma}^{R,h})). \quad (8.38)$$

## 8.4 A “total” orthogonal sum

Clearly, for the class of problems under consideration, solutions must be generated numerically, for example, as in the last section, by the finite element method. We now consider the effect of the use of the finite element method to generate a subsatial approximation to  $\tilde{\mathbf{u}}$ , denoted  $\tilde{\mathbf{u}}^h$ , governed per subdomain by

Find  $\tilde{\mathbf{u}}_K^h \in \mathbf{H}_u^h(\Omega_K) \subset \mathbf{H}^1(\Omega)$ ,  $\tilde{\mathbf{u}}_K^h|_{\partial\Omega_K \cap (\Omega \cup \Gamma_u)} = \mathbf{U} \in \mathbf{H}^1(\Omega)$ , such that

$$\int_{\Omega_K} \nabla \mathbf{v}_K : \tilde{\boldsymbol{\sigma}}_K^h \, d\Omega = \int_{\Omega_K} \mathbf{f} \cdot \mathbf{v}_K \, d\Omega + \int_{\partial\Omega_K \cap \Gamma_t} \mathbf{t} \cdot \mathbf{v}_K \, dA$$

$\forall \mathbf{v}_K^h \in \mathbf{H}_v^h(\Omega_K) \subset \mathbf{H}^1(\Omega_K)$ ,  $\mathbf{v}_K^h|_{\partial\Omega_K \cap (\Omega \cup \Gamma_u)} = \mathbf{0}$ .

(8.39)

A critical point is that  $\mathbf{H}_u^h(\Omega)$ ,  $\mathbf{H}_v^h(\Omega) \subset \mathbf{H}^1(\Omega)$ . This “inner” approximation allows the development of a straightforward decomposition. Using a subsatial approximation, by direct expansion we have

$$\begin{aligned} \mathcal{J}(\tilde{\mathbf{u}}^h) &= \sum_{K=1}^N \mathcal{J}_K(\tilde{\mathbf{u}}_K^h) = \sum_{K=1}^N \mathcal{J}_K(\tilde{\mathbf{u}}_K + (\tilde{\mathbf{u}}_K^h - \tilde{\mathbf{u}}_K)), \\ &= \sum_{K=1}^N \mathcal{J}_K(\tilde{\mathbf{u}}_K) + \sum_{K=1}^N \int_{\Omega_K} \nabla(\tilde{\mathbf{u}}_K^h - \tilde{\mathbf{u}}_K) : \mathbf{IE} : \nabla \tilde{\mathbf{u}}_K \, d\Omega, \end{aligned}$$